VERIFICATION OF PROPOSED AASHTO PERFORMANCE MODEL

Improved Consideration of Support in AASHTO Methodology

A comprehensive evaluation of the AASHO Road Test and the resulting concrete pavement design models conducted under NCHRP 1-30 revealed several major deficiencies related to pavement support conditions. Due to the nature of these deficiencies, a major effort was expended to develop procedures for improved consideration of support into the AASHTO design methodology. Details of the development are given in Appendix E of Reference 2.

This effort required an extensive examination of the design and subsequent performance of the test pavements at the AASHO Road Test site, a detailed examination of the original development of the concrete pavement design model and its subsequent "extensions" over time, the formulation of recommended improvements for pavement support, and, finally, the incorporation of these improvements into a proposed revision to the AASHTO design model with different support inputs. Efforts were then made to verify the proposed revised AASHTO design model using long-term performance data from the extended AASHO Road Test and other in-service pavements in a variety of climatic zones. The proposed revisions to the relevant portions of the AASHTO Guide are provided in the appendix.

Deficiencies in 1993 AASHTO Procedure Related to Pavement Support

The following summary is a list of the specific deficiencies in the current version of the AASHTO design procedure for concrete pavements that are related to pavement support.

- The gross k-value input assumes a large amount of permanent deformation and does not represent the support that the pavements actually experience during traffic loading. An elastic k-value provides a far more realistic match to measured strains. In analysis of AASHO Road Test pavements, the elastic k-value was found to reduce the stress in the slab equal to that computed from measured strains under creep speed axle loading.

- The lowest gross k-value that was measured on top of the base during the spring (60 psi/in [16 kPa/mm]) was incorporated into the AASHTO model in 1961 and has not been changed. The 1986 version provided a procedure to consider seasonal variation in selection of a design k-value; however, the design equation was not modified to incorporate the effective k-value that existed at the Road Test site. Thus, the current seasonal adjustment procedure is incompatible with the current design model.

- The effect of the base course on performance is not properly considered through the composite "top of the base" k-value. This is especially true for stiff treated bases that act as structural layers in reducing stress in the slab. An improved way to model the effect of the base layer on slab stress is needed.

- Substantial loss of support existed for many sections at the AASHO site, which led to increased slab cracking and loss of serviceability; thus, the performance data and design

equation already incorporate considerable loss of support. Incorporation of an additional loss of support factor results in overdesign. What is needed is a way to consider the benefit of an improved base on performance in terms of cracking and faulting.

- The 1961 extension used Spangler's unprotected corner equation. The critical stress location at the AASHO Road Test was along the slab edge for slabs 6.5 in [165 mm] and greater, and resulted in transverse fatigue cracks initiating at the bottom of the slab. The stresses in the vicinity of the corner were much lower than those at midslab due to the well-doweled joints. Use of Spangler's corner equation with doweled joints does not model the critical stress and crack initiation location, and thus cannot possibly provide accurate indications of the effect of slab support on cracking, especially when thermal curling and moisture warping are considered.

- The current AASHTO procedure does not provide a methodology to design a pavement with undoweled joints. The J factor only considers tensile stress that controls cracking, not faulting. An undoweled joint requires improved slab support from the base and a more erosion-resistant base material to prevent loss of support over time and premature failure. Thermal curling and moisture warping, which become much more critical to performance with undoweled joints, are not considered in the current AASHTO procedure.

- Joint spacing other than that of the Road Test slabs is not considered at all in the current design procedure. It is known from many other studies that joint spacing has a major effect on slab cracking and faulting.(10,11) Subgrade and base support interact with joint spacing to affect combined slab stresses from load, temperature, and moisture gradients. Thus, slab support is a very important variable in the selection of joint spacing to minimize transverse cracking.

- The original 1961 model reflects the climate of the AASHO Road Test site only. The 1993 version does not include any variable that adjusts for different climates. Thus, other climates that cause different magnitudes of slab curling or warping cannot be considered. This limitation alone has led to many pavement failures from premature cracking.

- The only distress manifestation considered directly by the design procedure is transverse slab cracking, because that is basically the only distress that occurred at the Road Test (other than erosion and loss of support that contributes to slab cracking). Thus, the loss of serviceability was due almost entirely to slab cracking and the subsequent deterioration of those cracks, resulting in roughness and loss of serviceability. Some sections had excessive loss of support prior to failure from slab cracking. Cracking is related to slab support, and the Spangler corner equation incorporated into the AASHTO design equation is not a realistic model for predicting the cracking that occurred, as noted above.

- Faulting of transverse joints did not occur during the 2 years of the Road Test because the joints all had dowels; thus, the performance predicted by the design model does not consider the effect of faulting on loss of serviceability. The J factor, often thought to control faulting, has nothing to do with joint faulting.

- Although thermal curling and moisture warping of slabs occurred during the 2-year Road Test, the effects of these important factors were not considered in any of the extensions. This is important because any design feature that would increase stresses from either of these actions cannot be considered in the design of that pavement. For example, joint spacing, base stiffness, and subgrade stiffness all affect stresses from thermal curling and moisture gradients through the slab. None of these can be considered in pavement design using the current AASHTO Guide procedure.

The following sections briefly summarize the efforts made for NCHRP 1-30 to develop an improved methodology for consideration of slab support in the AASHTO design procedure.

Improved AASHTO Methodology Recommended

Improved technology exists today that was not available in 1961, including the capabilities of three-dimensional finite element models to compute slab stresses, larger and faster computers, and advanced mechanistic and statistical modeling. This technology was applied to the original AASHO model to develop an extended and improved design model for concrete pavements that more fully considers pavement "support" aspects. Specific improvements in the proposed revision to the AASHTO design procedure include the following:

1. Defining the k-value specifically as the value determined on the finished roadbed soil or embankment, upon which the base and slab will eventually be constructed. A composite "top of the base" k-value is not valid and is not recommended for design.

2. The k-value input recommended is the elastic k-value as tested extensively at the AASHO Road Test and similarly at the Arlington, Virginia, test site. The elastic k-value was found to result in slab stresses similar to those produced in the field by axle loads at creep speed.

3. Seasonal support variations are considered through the determination of an effective yearly elastic k-value of the embankment/subgrade. A procedure was developed to determine the effective k-value for the design.

4. The effect of the base course on slab stress due to load and temperature and moisture gradients is directly considered. The base thickness, stiffness, and friction coefficient (between the slab and the base) are direct inputs to the design procedure.

5. Temperature gradients and moisture gradients (as equivalent temperature gradients) are directly considered as inputs to the design procedure.

6. A procedure was developed for checking joint faulting and adjusting joint design if deficient, rather than increasing slab thickness.

7. Joint spacing is directly considered through its interaction with slab support and effect on combined load and temperature curling stresses.

8. The effects of longitudinal edge load transfer or a widened traffic lane on critical stress reduction are considered directly.

9. Joint (corner) load position stresses are checked for undoweled joints in slab design.

A new design model for concrete pavement design was developed using the same general approach used in 1961 to extend the original empirical model and also incorporate the above capabilities. Figure 23 shows this mechanistic-empirical type of model, in which log W is linearly related to the logarithm of the strength-to-stress ratio S'_c / σ. The new concrete pavement log W model (for 50 percent reliability) was obtained by combining the empirical model and the mechanistic-empirical model as follows:

$$\log W' = \log W + \left(5.065 - 0.03295\ P2^{2.4} \right) * \left[\log \left(\frac{(S'_c)'}{\sigma'} \right) - \log \left(\frac{S'_c}{\sigma} \right) \right] \quad [20]$$

where W' = number of design 18-kip [40-kN] ESALs in traffic lane
σ' = maximum tensile slab stress for the midslab load position due to combined load and effective temperature curl (with inputs for the new pavement design)
W = number of 18-kip [40-kN] ESALs estimated using the original empirical AASHO design model from the main loops (with inputs from original AASHO Road Test)
σ = maximum tensile slab stress for the midslab load position due to combined load and effective temperature curl (with inputs from original AASHO Road Test)

The above equation represents the best fit relationship between design features and log W. Reliability can be added in a manner similar to that in the current AASHTO Guide.

Field Verification of New Models

Data were obtained from the 14-year extended AASHO Road Test (12) and the RPPR database (11). This database provides performance data from sections with various base types, subgrades, climates, and designs from many States. The number of 18-kip [40-kN] ESALs (log W) was predicted from the initial serviceability (P1) to the current serviceability (P2). The actual number of ESALs was computed from the traffic data on each section. The results shown in Figure 24 indicate a reasonable prediction of log W for a wide variety of pavement designs across the United States, with no particular bias of overprediction or underprediction. However, the data are very limited, and additional data are needed for verification. Such data are available in the LTPP database.

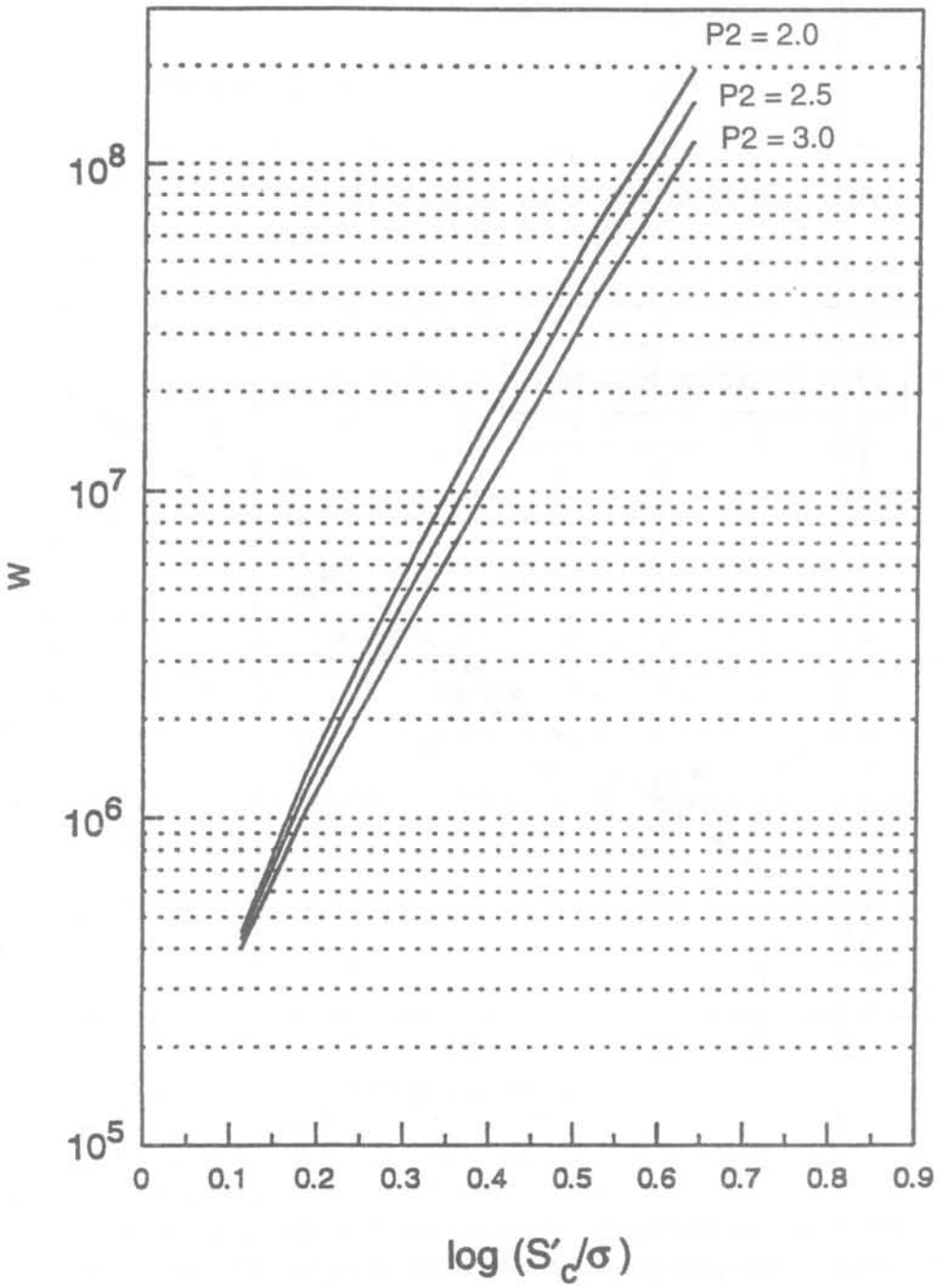

Figure 23. Relationship of W to log S'_c/σ for three terminal serviceability levels for the proposed revised AASHTO extended concrete pavement design model.

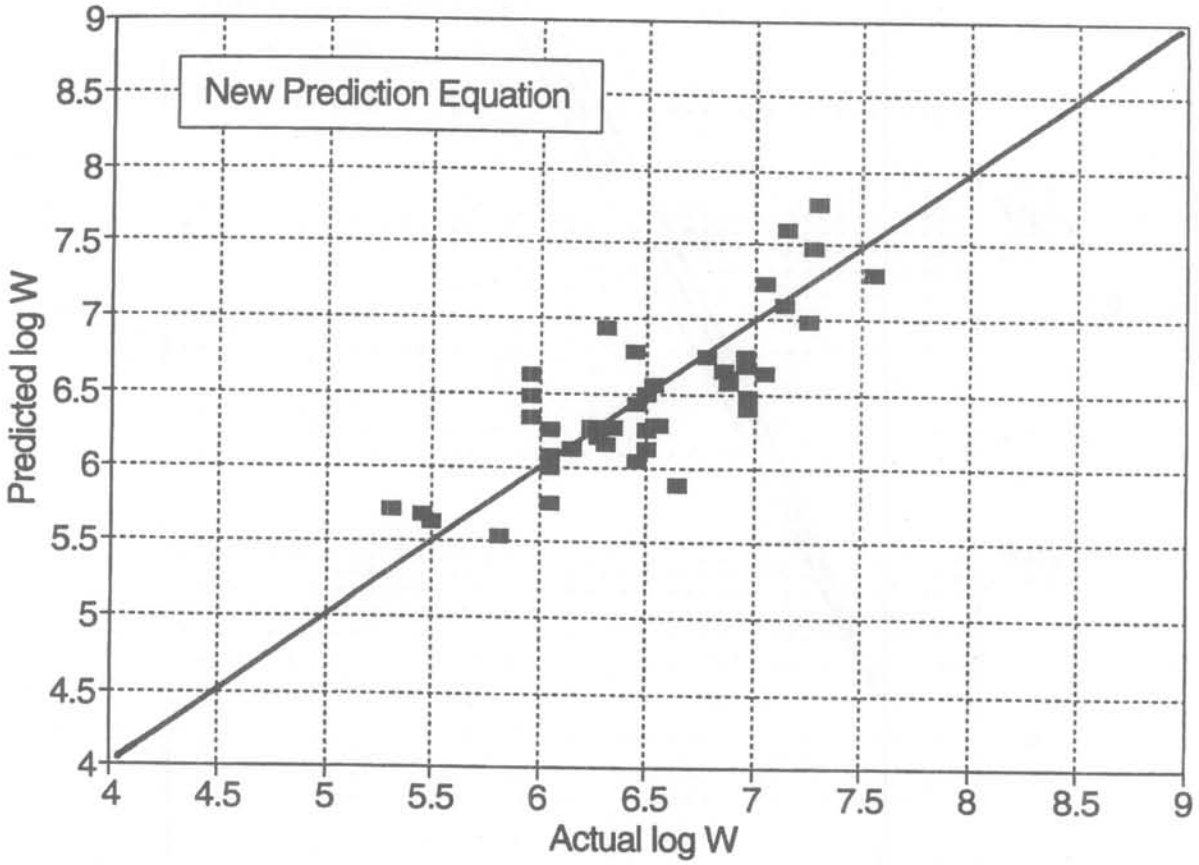

Figure 24. Predicted versus actual log W for test sections from the extended I-80 tests and the FHWA database, using the proposed revised concrete pavement design model.

Validation of Design Model With LTPP Data

Data were extracted from the LTPP database from GPS-3, -4, and -5 experiments for the purpose of validating the new design model. The data were stored in a spreadsheet format for the convenience of data manipulation, plotting, and analysis. The data items listed below were required for the analysis. Where necessary, information about the selection and use of the available data is provided as well.

Strategic Highway Research Program (SHRP) ID and State Code
Year opened to traffic

Accumulated ESALs—Annual ESALs were obtained for every section and plotted versus time. A best fit regression curve was fitted through the data. Some of the data were highly variable. The total accumulated ESALs were summed for each year, from the year of opening to traffic to the prediction year (the year for which an IRI was selected to estimate the serviceability, as described below. ESAL data were missing for several sections. For each section for which ESAL data were analyzed, the quality of fit of the ESAL projection curve to the available data was characterized by an R^2. When the analysis spreadsheet for the GPS-3 sections was fully assembled and predicted log W from opening to the prediction year could be compared to the actual log W, no trend was apparent in the ratio of predicted to actual log W with respect to the R^2 of the ESAL prediction, as Figure 25 shows. Thus, no sections were removed from the analysis on the basis of the quality of the ESAL prediction.

IRI—IRI data measured between 1989 and 1993 were retrieved and plotted for every individual section. The IRI that best appeared to represent the value in 1992 or 1993 was determined from the graphs for each section. In a very few cases, a dramatic drop in IRI was seen in one of these years, suggesting that perhaps the section received an overlay or other significant ride quality improvement. In these cases, the year of the last IRI value measured before the significant drop was selected as the prediction year. IRI data were missing for several sections.

Joint faulting—Measured faulting at the slab edge (0.3 m) and in the wheel path (0.75 m) were retrieved and plotted over time. Data were missing from several sections and the data were very erratic from year to year. Faulting values corresponding to the IRI year were selected for each section. In general, the edge faulting measurements were used, except for three sections for which the edge data were not available, but the wheelpath data were. Negative faulting values were assumed to be zeros. Sections that had no faulting data were excluded from the analysis because the correction to the serviceability loss cannot be done without knowing the faulting magnitude.

Present Serviceability Index (PSI)—The PSI was estimated from the IRI (inches/mile) using the following equation (13):

$$PSI = 5\, e^{(-0.0041\ IRI)} \qquad [21]$$

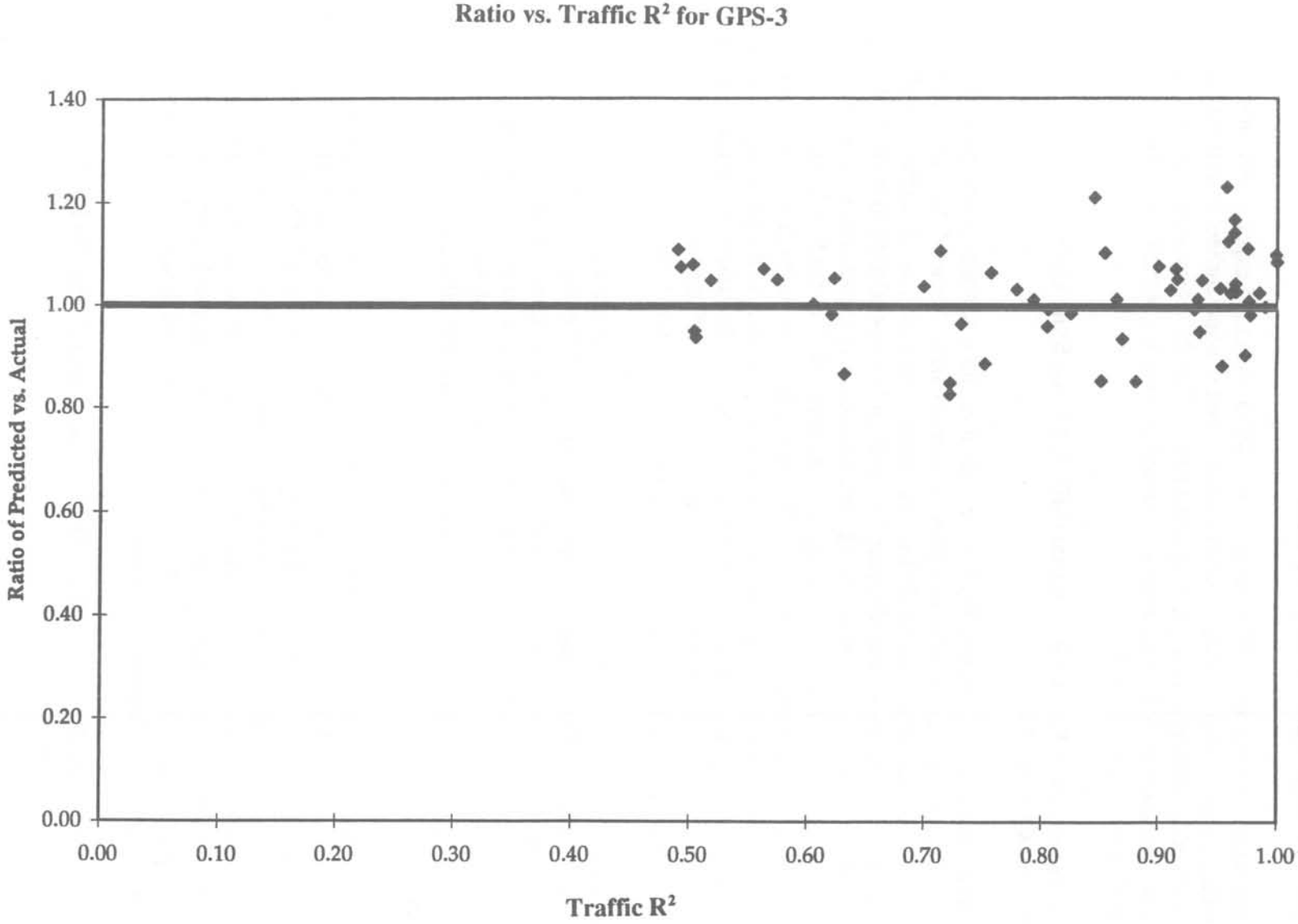

Figure 25. Ratio of predicted vs. actual log W versus ESAL prediction accuracy.

Adjusted PSI for zero faulting—The original AASHO Road Test included well-doweled joints that did not fault during the 2-year study. Thus, the new model, which is based on the original AASHTO model, is only valid for pavements that do not fault. Thus, an adjustment was necessary for the LTPP sections that had measurable faulting. The following adjustment was made that essentially increased the PSI computed directly from the IRI, depending on the amount of faulting.

For example, suppose that a section had an IRI of 81 in/mi [1278.18 mm/km] in 1993, which corresponds to an estimated PSI of 3.59, and suppose also that the section has 1.15 mm of faulting, which corresponds to an IRI of 21.5 in/mi [339.27 mm/km]. The IRI without faulting would then be 81 - 21.5 = 59.5 in/mi [938.91 mm/km]. The PSI estimated from this IRI only is 3.92. In other words, the actual serviceability in the prediction year is increased to remove the portion of the serviceability loss that is due to faulting.

Initial PSI — Since most of the LTPP sections were several years old at the time of the first IRI measurement, there is no way to estimate their initial PSI. This is particularly true for the specific 500-ft [152-m] LTPP section. Based on information obtained from state highway agencies during the early analysis contract (16), a value of 4.25 was used for all sections, recognizing that the true value ranges in practice (prior to smoothness specifications at least) from 3.5 to 4.8. Also, a sensitivity analysis is conducted to show its relative impact.

Slab thickness — Data from cores were used. If these were not available, inventory data were used.

Average transverse joint spacing — If the pavement had a random joint spacing, the average was computed and used in the analysis.

Concrete slab flexural strength — The required input is 28-day, third-point loading, mean flexural strength. This value had to be estimated from several different types of strength data available:

(1) Indirect tensile strengths from 6-in- [15-cm-] diameter cores that were cut from the sections were obtained from the database. The flexural strength was estimated using the following relationship developed by Hammitt (14):

$$FS = 1.02\ ST + 210 \qquad [22]$$

where FS = flexural strength in third-point loading, psi
ST = split tensile strength, psi

The flexural strength estimated from this equation using core split tensile strength represents the pavement at the time the core was taken. This strength had to be adjusted to an estimated 28-day strength for use in the design model. A model developed under the Federal Highway Administration (FHWA) Zero-Maintenance study (15) was used to predict the 28-day strength from the strength at any other time:

$$R = 1.22 + 0.17 \log10\ t - 0.05 (\log10\ t)^2 \quad [23]$$

where R = ratio of flexural strength at time t to flexural strength at 28 days
t = time from placement, years

For example, a flexural strength obtained at 20 years of 800 psi [5.5 MPa] would result in an estimated flexural strength of 590 psi [4.07 MPa] at 28 days.

(2) If the core strength was missing, the database was searched for inventory data for flexural strength or compressive strength. If 14-day strengths were available, they were increased by 10 percent to estimate 28-day strengths. If 7-day strengths were available, they were increased by 30 percent to estimate 28-day strengths. Very often, the available inventory flexural strength values were very high.

(3) If none of the above data were available, the mean flexural strength (650 psi [4.48 MPa]) was used for the section.

(4) The above values were reviewed for either very low values or very high values. A practical range of 500 psi [3.45 MPa] minimum to 800 psi [5.5 MPa] maximum was allowed into the analysis. Any values outside of these limits were not used, and the mean value of 650 psi [4.48 MPa] was used.

Concrete slab elastic modulus — The static modulus was estimated from the core compression tests.
Concrete slab Poisson's ratio — These data were obtained mostly from core testing data. If the value was not available, a value of 0.20 was assumed.
Base type — Information was obtained from the database.
Base thickness — Data were obtained from the coring data.
Base elastic modulus — The static modulus was estimated from experience based on the description of the base material.
Slab/base coefficient of friction — Estimated from NCHRP 1-30 published summary of testing data.
Subgrade elastic static k-value — Backcalculated from FWD data and divided by 2.00. Note: This is essentially the k-value of the underlying subgrade as required input by NCHRP 1-30.
Edge support adjustment factor — Based on NCHRP 1-30 recommendations, this value is a fraction by which the free edge stress is multiplied. For a free edge (AC shoulder), this value is 1.00; for a tied PCC shoulder, it is 0.94; and for a widened traffic lane, it is 0.92. Note that the axle load is not located at the edge of the slab, but it is approximately in the center of the wheel path and this is the reduction factor for that location only.
Mean annual air temperature — Obtained from the LTPP database.
Mean annual precipitation — Obtained from the LTPP database.
Mean annual wind speed — Obtained from maps of the United States published by the National Oceanic and Atmospheric Administration (NOAA).

Effective positive daytime temperature gradient — Computed according to NCHRP 1-30 model, using mean annual temperature, precipitation, and wind speed.
Predicted ESALs carried over PSI loss from PSI initial to PSI in 1992 or 1993 when latest IRI was measured — This value was computed using the NCHRP 1-30 new design model with all of the above inputs.
Actual ESALs carried since opening to traffic — Estimated as previously described for each year and accumulated to the prediction year (1992 or 1993).

Performance Prediction Capability of Proposed New Model

After all of the needed data were assembled and checked, the predicted log W was compared to the actual log W for each section over various categories of the data, as described below. There are two important aspects to this comparison: (1) magnitude of the differences section by section between predicted log W and actual log W, and (2) overall bias of the model to, on average, either overpredict or underpredict the actual log W. Both of these aspects are addressed in this section over the three main LTPP rigid pavement experiments of GPS-3, GPS-4, and GPS-5.

Performance Prediction for GPS-3 (JPCP)

Effect of initial serviceability. The prediction quality of the new model using initial serviceabilities of P1 = 4.5, 4.25, and 4.0 is illustrated in Figures 26, 27, and 28, respectively. The model overpredicts with P1 = 4.5, as seen in Figure 26 and in the paired two-tail t-test results summarized in Table 7. The null hypothesis is that the mean difference in predicted and actual log W is equal to zero, and the alternate hypothesis is that it is not equal to zero (the model could overpredict or underpredict log W). Since the computed t(2.49) is greater than the critical t(2.01) at the 0.05 level of significance, the null hypothesis is rejected at the 0.05 level of significance. There is a 0.016 probability of observing this large of a difference given that the null hypothesis is true. Thus, in engineering terms, the mean difference between predicted log W and actual log W values for GPS-3 sections is not zero when P1 = 4.5. The mean actual and predicted log W values are 6.65 and 6.82, respectively, which correspond to mean actual and predicted ESALs of 4.5 million and 6.6 million, respectively. The model overpredicts ESALs on average about 47 percent when the initial serviceability is estimated at 4.5.

Table 7. Actual versus predicted log W paired two-tail t-test results for GPS-3, P1 = 4.5.

Paired t-test for GPS-3 only (with P1=4.5) t-Test: Paired Sample for Means		
	Actual	Predicted
Mean (log W)	6.65	6.82
Variance	0.14	0.18
Observations	53	53
Hypothesized Mean	0	
df	52	
t Stat	-2.49	
P(T≤t) two-tail	0.016	
t Critical two-tail	2.01	

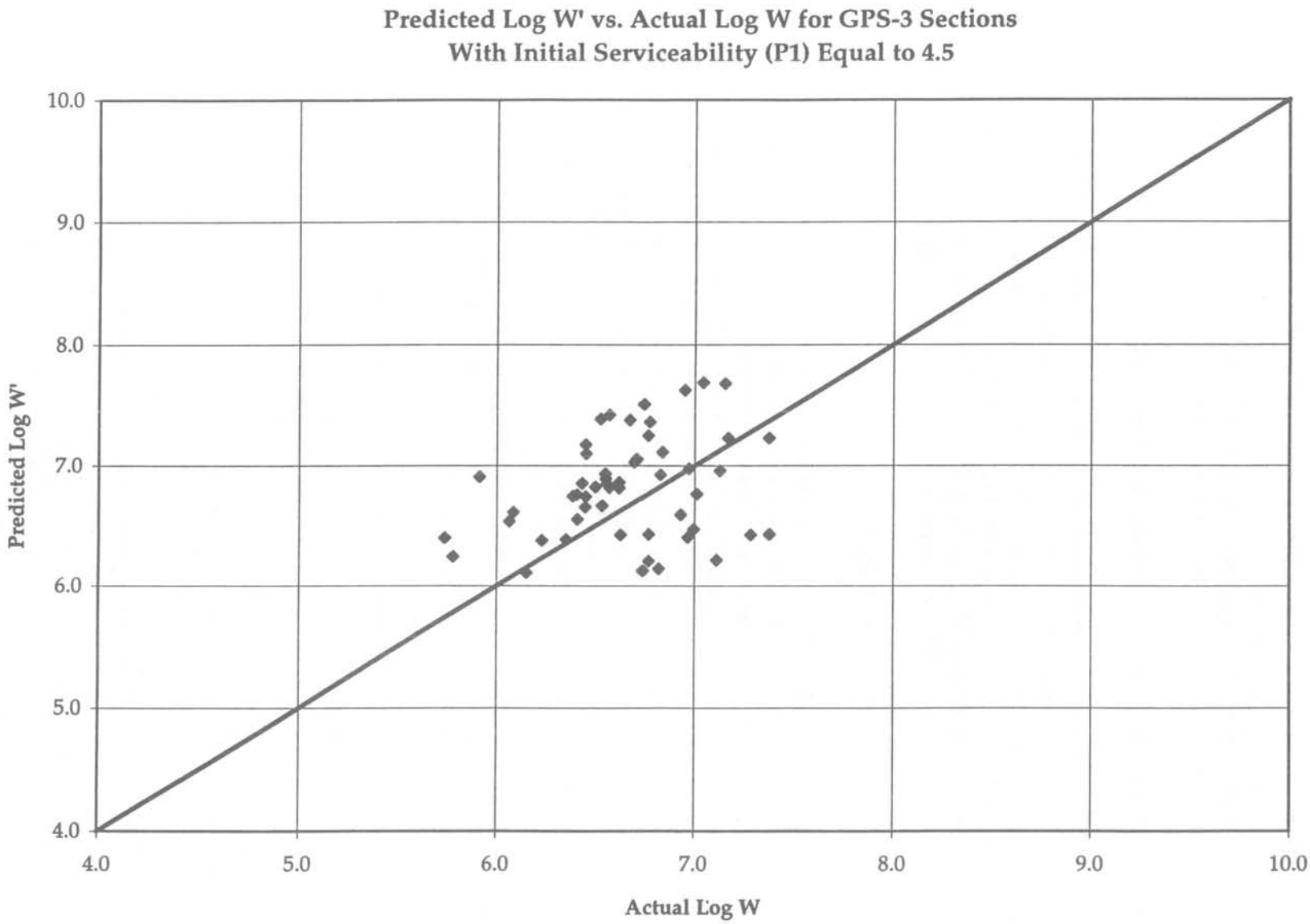

Figure 26. Predicted versus actual log W for GPS-3 using new model and P1 = 4.5.

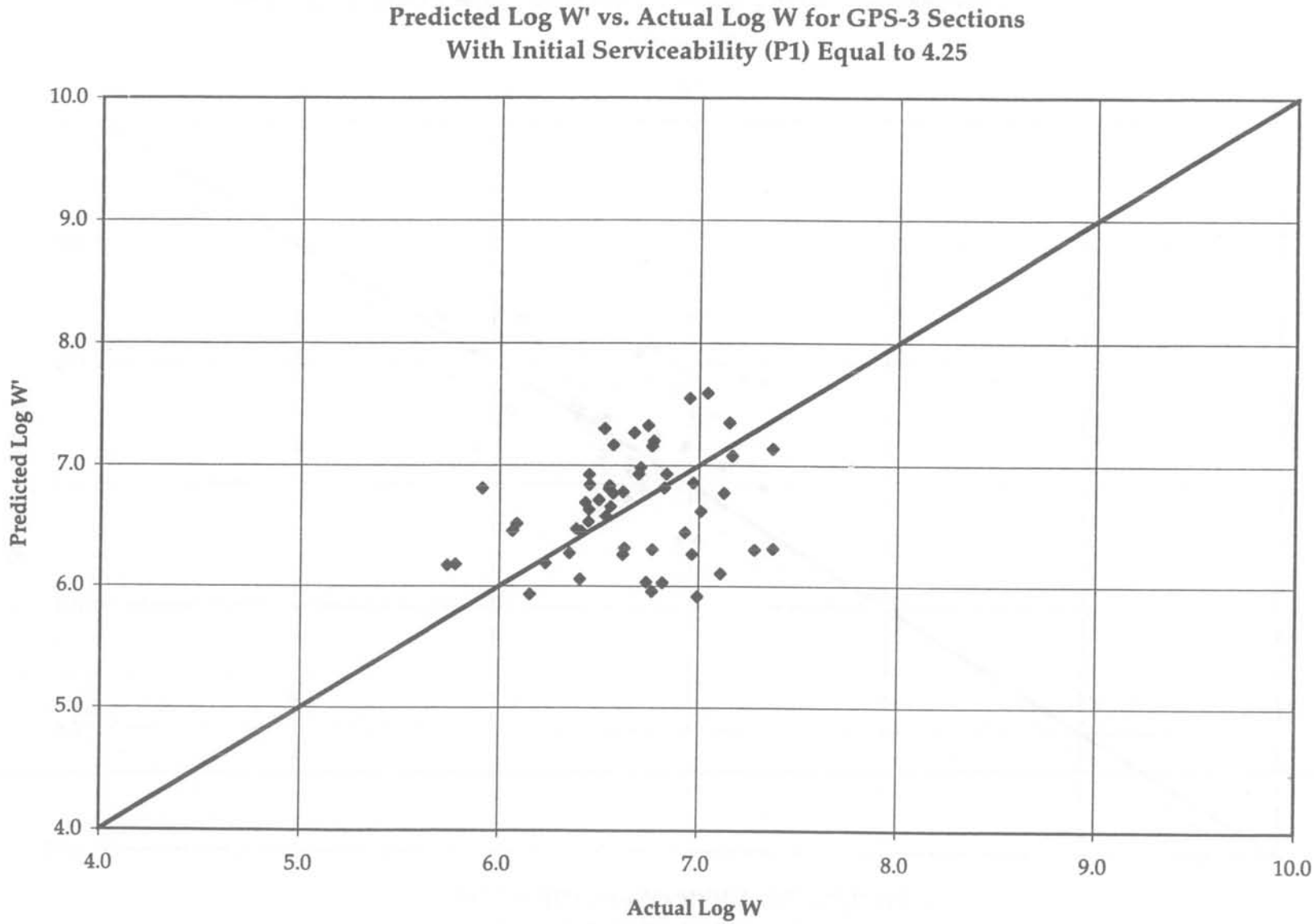

Figure 27. Predicted versus actual log W for GPS-3 using new model and P1 = 4.25.

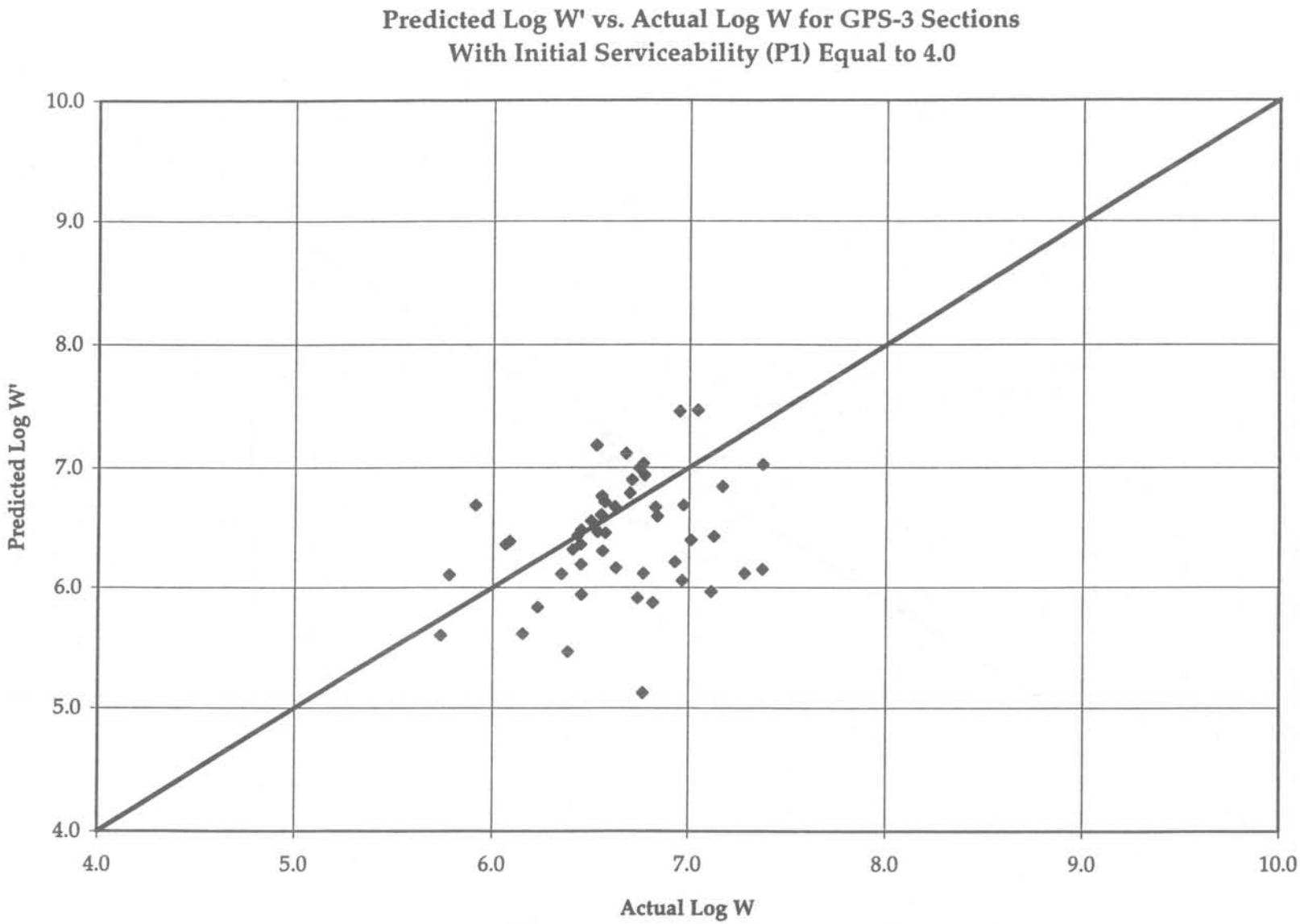

Figure 28. Predicted versus actual log W for GPS-3 using new model and P1 = 4.0.

When P1 = 4.25, results given in the paired t-test comparison in Table 8 and in Figure 27 show that there is no evidence on which to reject the null hypothesis that the mean difference between predicted and actual log W values are not zero. Both the mean actual and predicted log W values are 6.65, which correspond to mean actual and predicted ESALs of 4.5 million.

Table 8. Actual versus predicted log W paired t-test results for GPS-3, P1 = 4.25.

Paired t-test for GPS-3 only (with P1=4.25) t-Test: Paired Sample for Means		
	Actual	Predicted
Mean (log W)	6.65	6.65
Variance	0.14	0.19
Observations	53	53
Hypothesized Mean Difference	0	
df	52	
t Stat	-0.01	
P(T≤t) two-tail	0.99	
t Critical two-tail	2.01	

When P1 = 4.0, Table 9 and Figure 28 show evidence that the null hypothesis should be rejected at a significance level of 0.05 and the alternative hypothesis, being not equal to zero, should be accepted. The mean actual and predicted log W values are 6.64 and 6.42, respectively, which correspond to mean actual and predicted ESALs of 4.4 million and 2.6 million, respectively.

Table 9. Actual versus predicted log W paired t-test results for GPS-3, P1 = 4.0.

Paired t-test for GPS-3 only (with P1=4.0) t-Test: Paired Sample for Means		
	Actual	Predicted
Mean (log W)	6.64	6.42
Variance	0.14	0.24
Observations	49	49
Hypothesized Mean Difference	0	
df	48	
t Stat	2.89	
P(T≤t) two-tail	0.006	
t Critical two-tail	2.01	

Many of these sections were built in the 1960s and 1970s, long before smoothness specifications were used extensively. Thus, any initial serviceability values between 3.5 and 4.8 are possible. In any case, the significant effect of P1 on the overall prediction quality indicates that caution should be applied in drawing conclusions about predictive accuracy when the initial serviceability values are not known. All of the other analyses provided herein have been conducted at P1 = 4.25. This

is the value used in the LTPP early analysis work based on estimated initial serviceability values by the state highway agencies. (16)

Effect of slab thickness. The GPS-3 sections were separated into two groups: (1) 10 in [25 cm] or more thick and (2) less than 10 in [25 cm] thick. The prediction quality for the two groups may be seen in Figure 29. The paired two-tail t-test shows no evidence on which to reject the null hypothesis at either thickness level. Thus, the model produces unbiased predictions for either thinner or thicker slabs.

Effect of base type. The GPS-3 sections were also separated into two groups by base type: (1) those with granular bases and (2) those with treated bases (asphalt, cement, lean concrete). Based on the paired t-test results, there is no evidence on which to reject the null hypothesis for either granular or treated base types. This can be observed in Figure 30 where base type has no apparent effect on the prediction quality.

Effect of climatic zone. The GPS-3 sections are sorted into wet freeze, dry freeze, wet nonfreeze, and dry nonfreeze zones in Figures 31, 32, 33, and 34, respectively. Based on the t-test paired comparison, there is no evidence on which to reject the null hypothesis for any of the four climates.

1986 AASHTO model. Figure 35 shows the prediction quality of the 1986 AASHTO model when it is used to predict log W for all of the GPS-3 sections. The paired two-tail t-test results are shown in Table 10 for these data. The results show that there is no evidence on which to reject the null hypothesis, and that the mean difference between predicted and actual log W values is not zero.

Table 10. Paired two-tail t-test results for 1986 AASHTO model, GPS-3.

Paired t-test for GPS-3 only t-Test: Two-Tail Paired Sample for Means		
	Actual	Predicted
Mean (log W)	6.65	6.65
Variance	0.14	0.22
Observations	53	53
Hypothesized Mean Difference	0	
df	52	
t Stat	-0.01	
P(T≤t) two-tail	1.00	
t Critical two-tail	2.01	

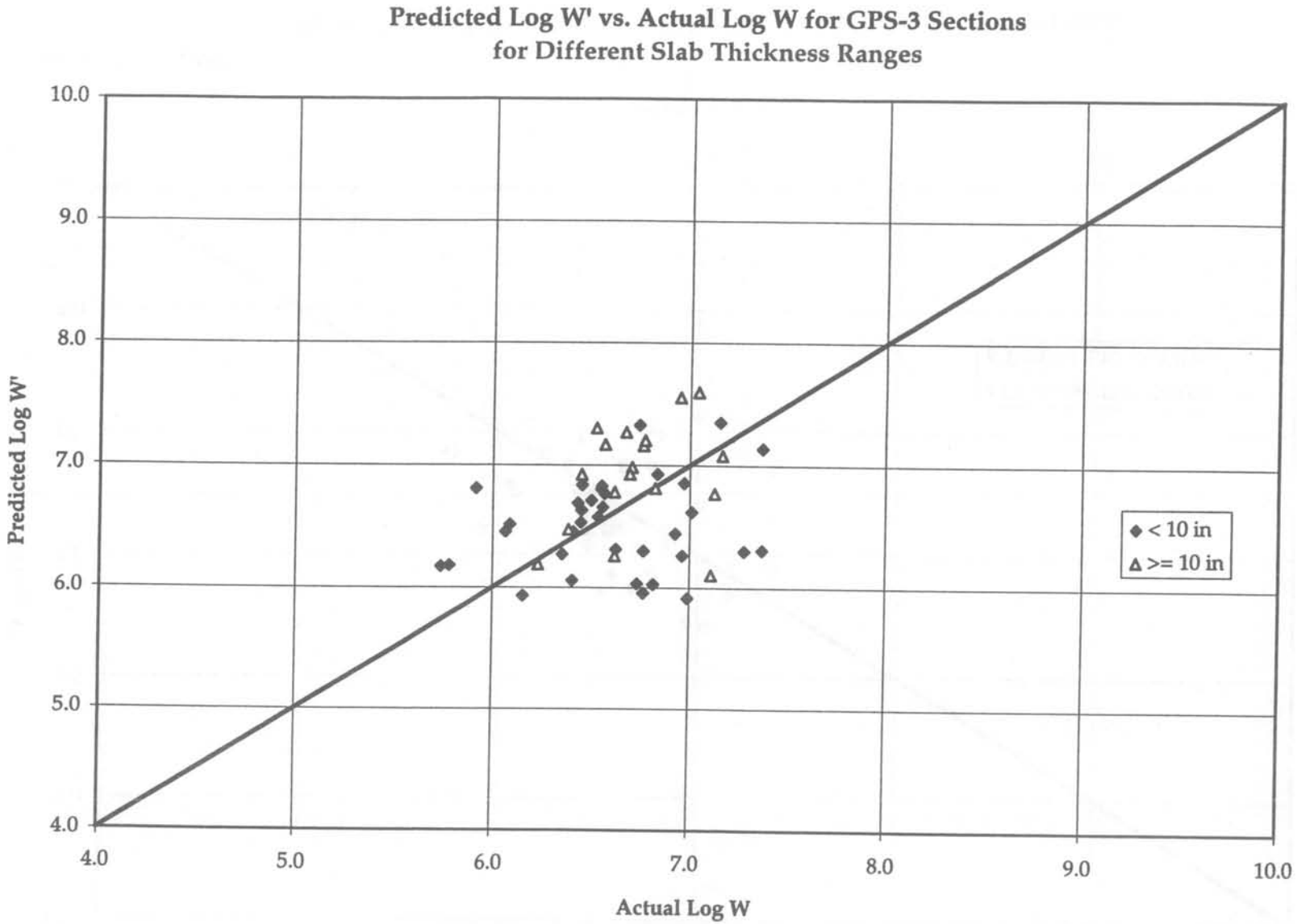

Figure 29. Predicted versus actual log W for GPS-3 slabs less than 10 in [25.4 cm] thick and greater than or equal to 10 in [25.4 cm] thick.

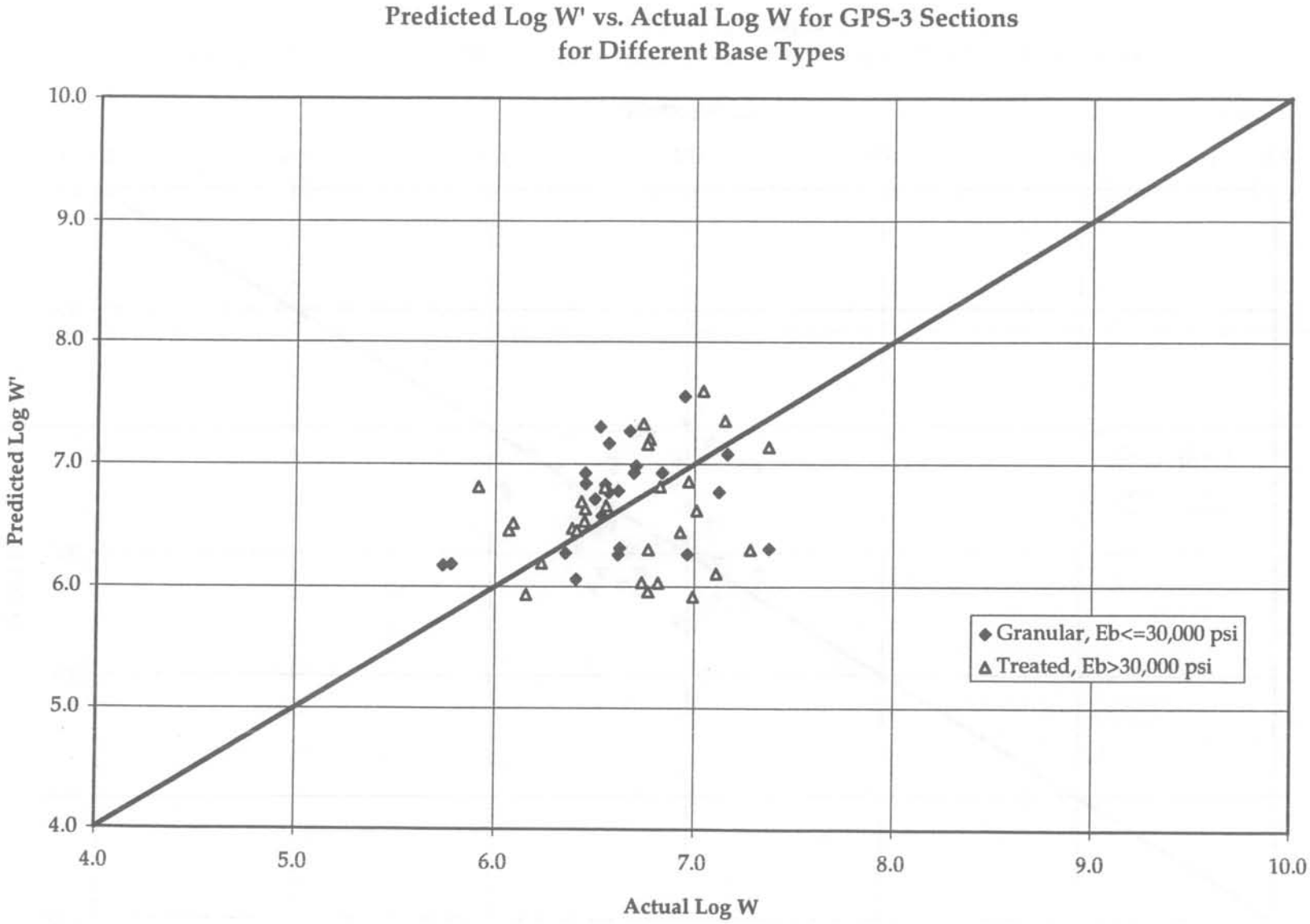

30,000 psi = 206.9 MPa

Figure 30. Predicted versus actual log W for GPS-3 with granular and treated bases.

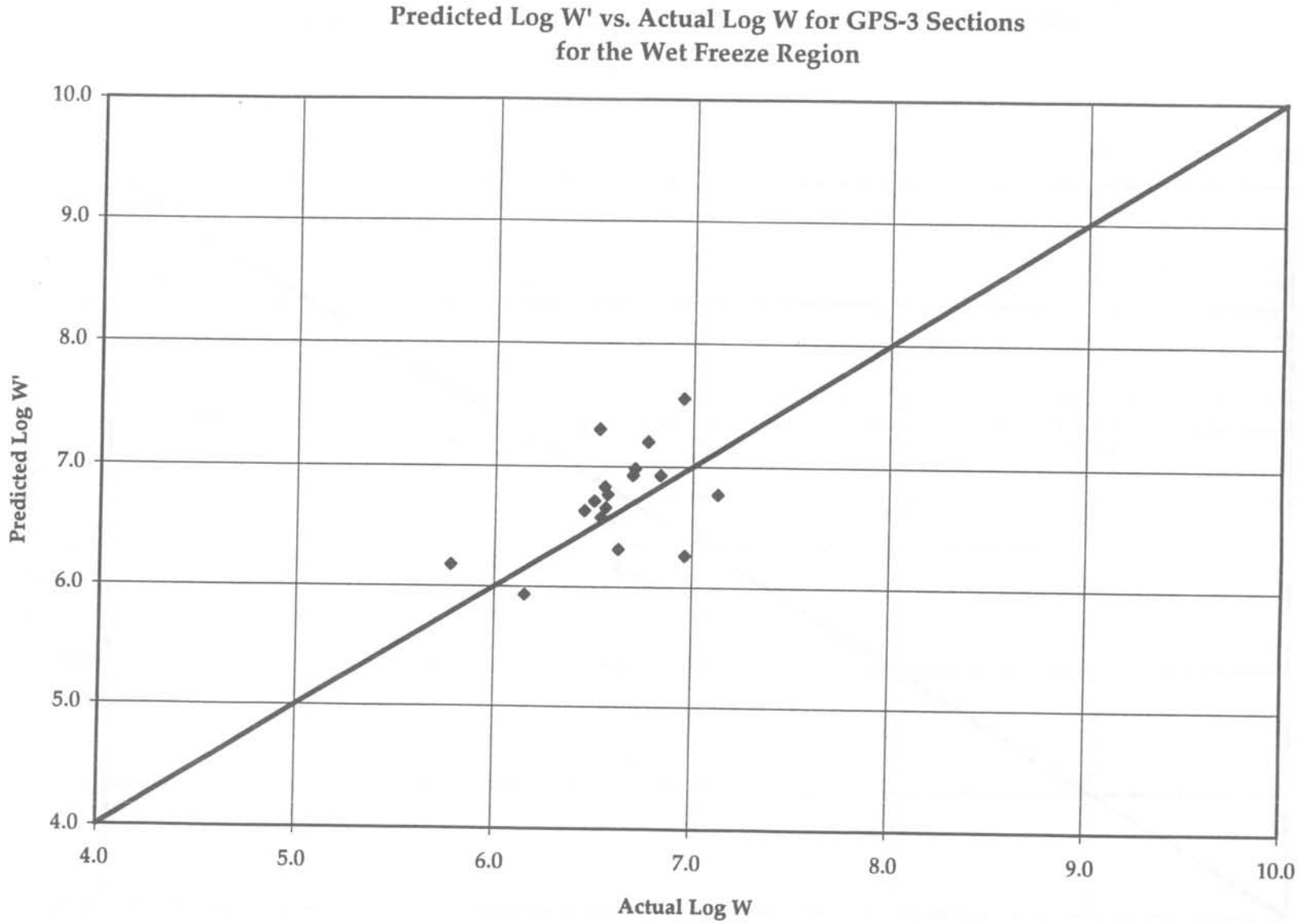

Figure 31. Predicted versus actual log W for GPS-3 in wet freeze climatic zone.

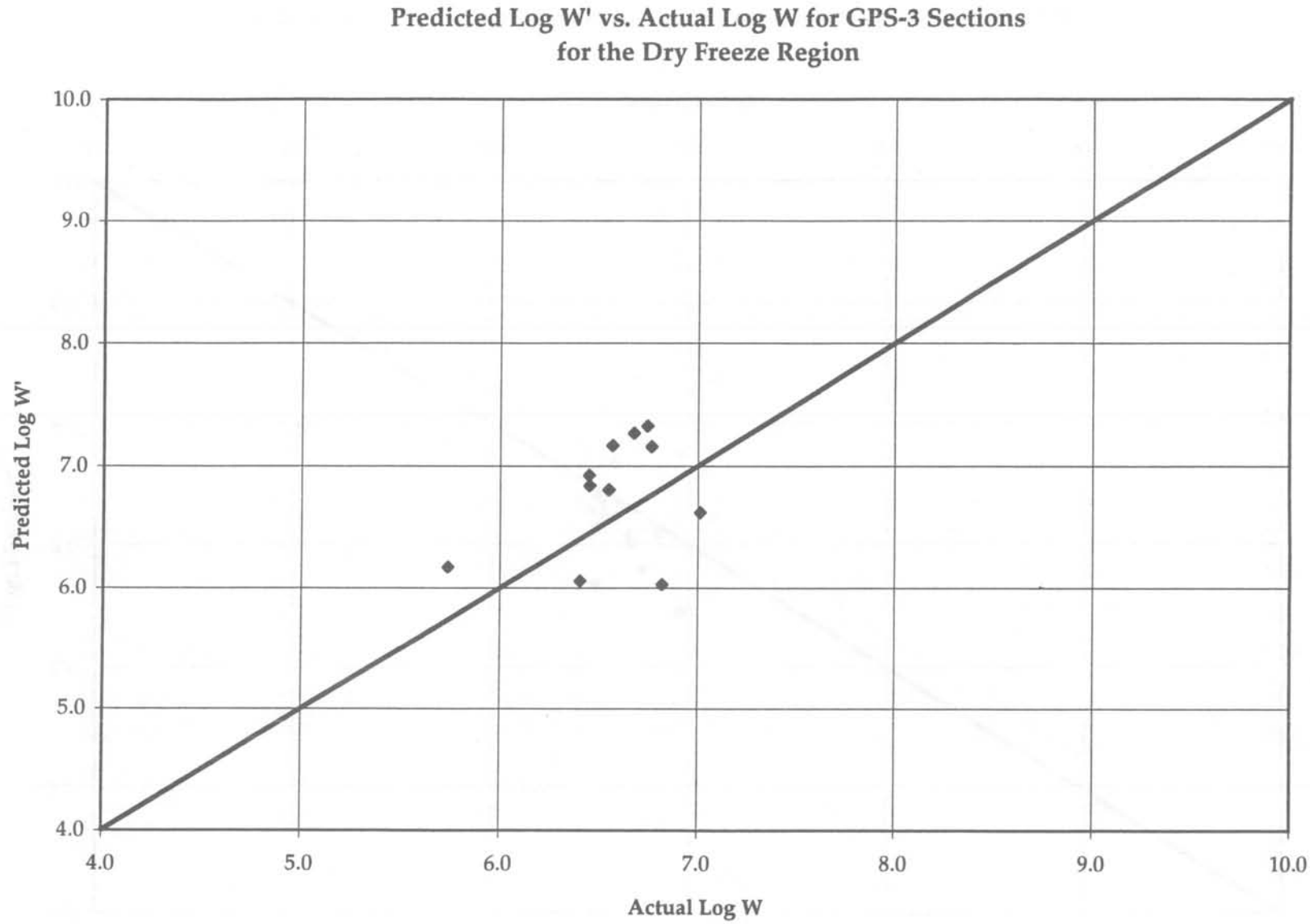

Figure 32. Predicted versus actual log W for GPS-3 in dry freeze climatic zone.

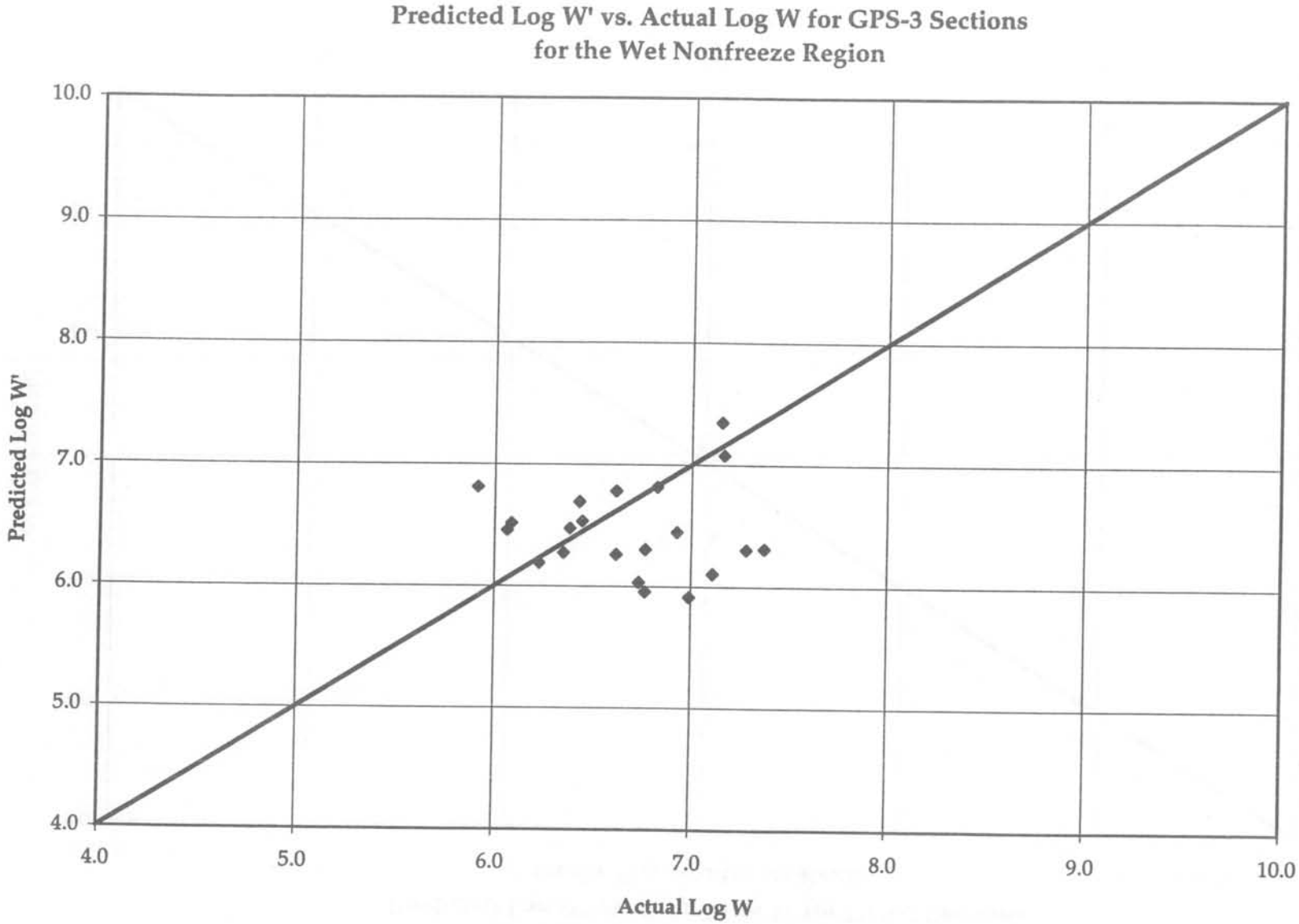

Figure 33. Predicted versus actual log W for GPS-3 in wet nonfreeze climatic zone.

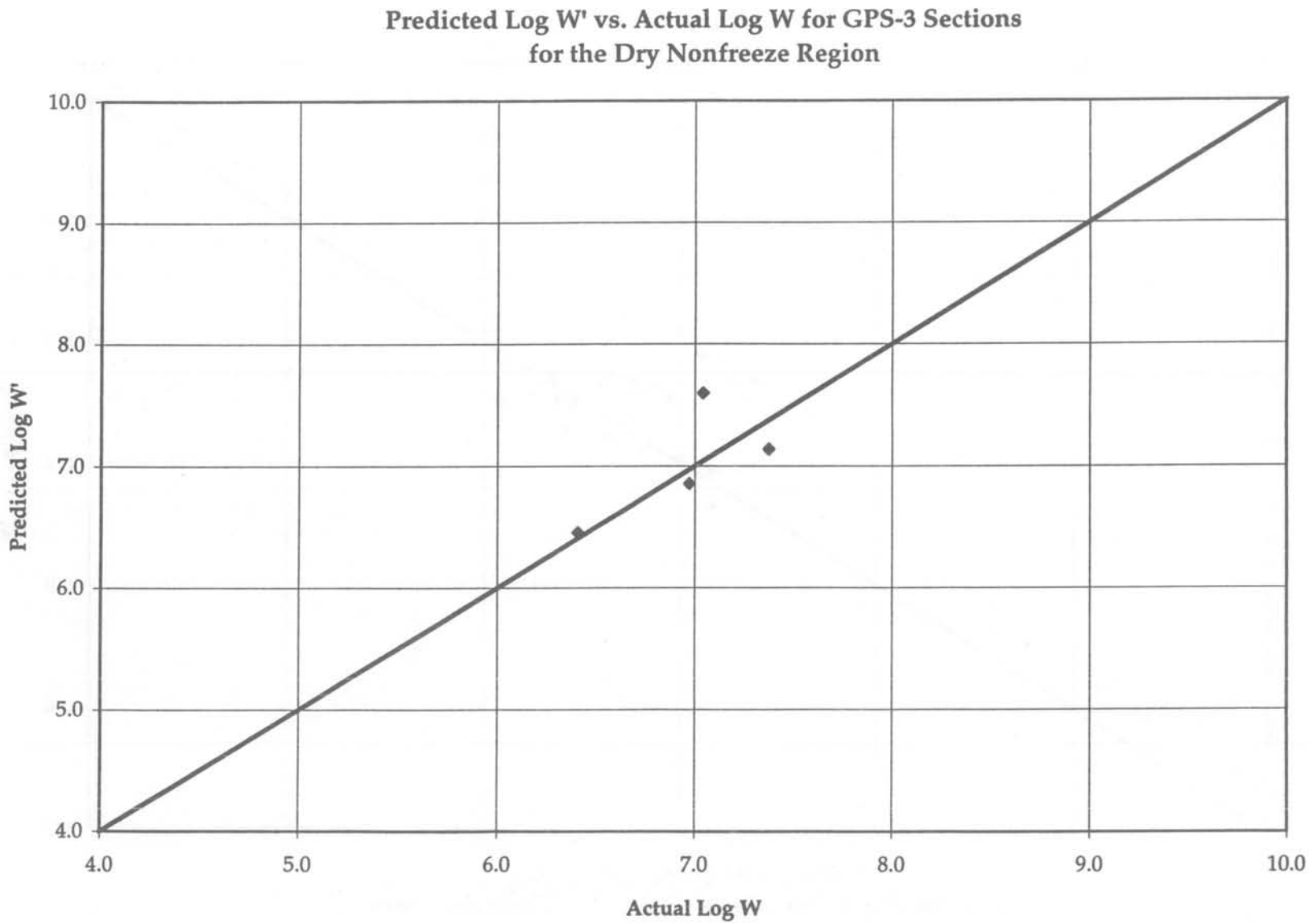

Figure 34. Predicted versus actual log W for GPS-3 in dry nonfreeze climatic zone.

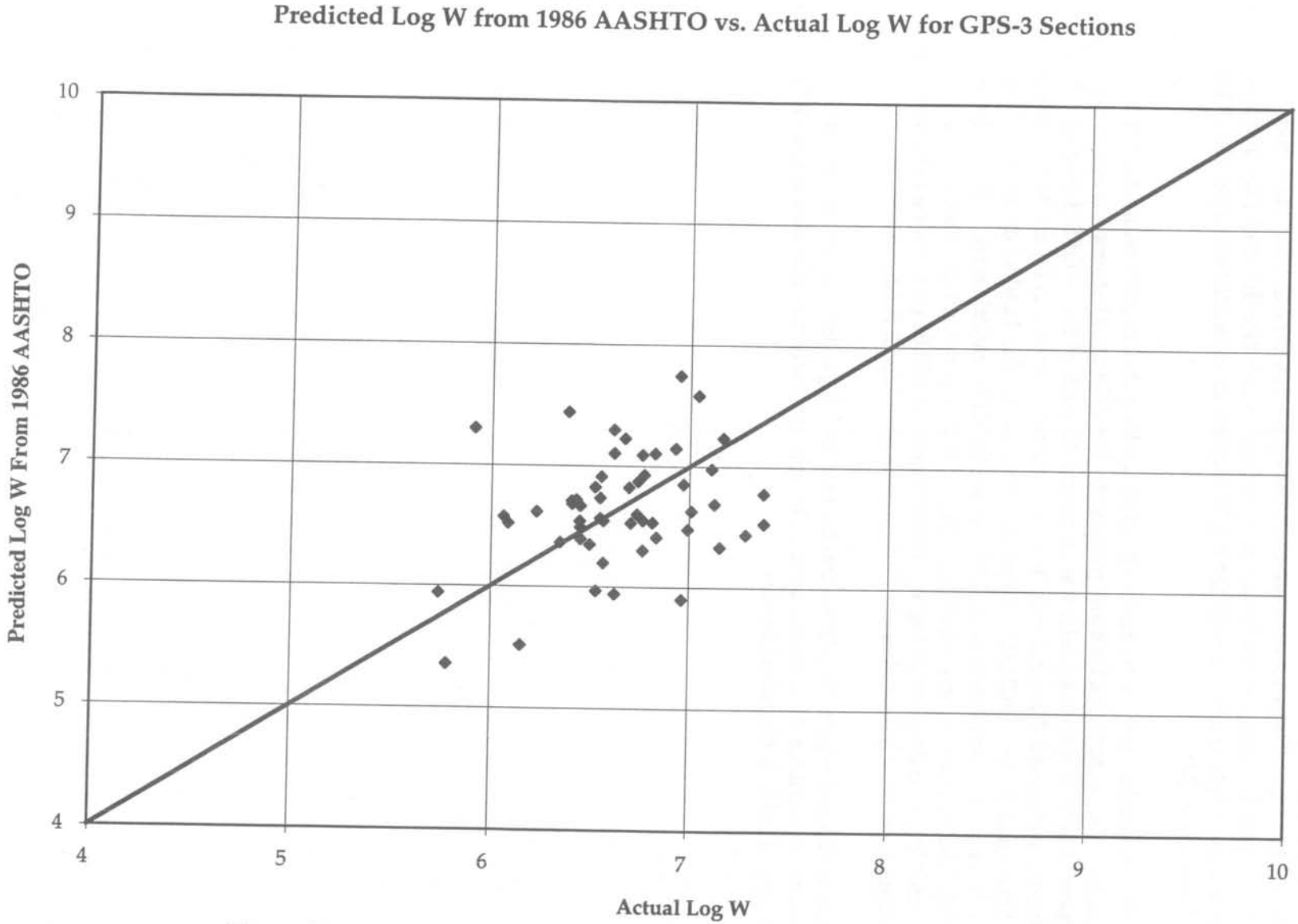

Figure 35. Predicted versus actual log W for GPS-3 using 1986 AASHTO model.

Comparison of 1986 AASHTO model with new NCHRP 1-30 model. The paired two-tail t-test results for the new NCHRP 1-30 model are shown in Table 8. These results provide no evidence that the null hypothesis should be rejected for this comparison. Thus, both of these models apparently have the ability to predict without bias (when the results are averaged over a large number of pavement sections) the log W required to reduce the initial serviceability from P1 to a lower value P2.

Another evaluation that can be made with each model is the accuracy with which it can predict the actual log W of a section of highway pavement. The difference between the actual log W and the predicted log W (for both models) was computed for each of the 53 GPS-3 sections. The distribution of these differences (which are logarithms) is shown in Figure 36 for both the 1986 AASHTO and the new NCHRP 1-30 prediction models. The standard deviations of the array of 53 differences for each model were 0.50 for the AASHTO model and 0.50 for the NCHRP 1-30 model. These values are important since they represent an overall difference between the predicted log W and the actual log W. More discussion will be provided on these values in a subsequent section entitled "Variability Components of Model Prediction."

These results and Figure 36 indicate that the two models predict with about the same overall accuracy, and that the differences appear to be approximately normally distributed (which is the assumption made in the paired t-tests).

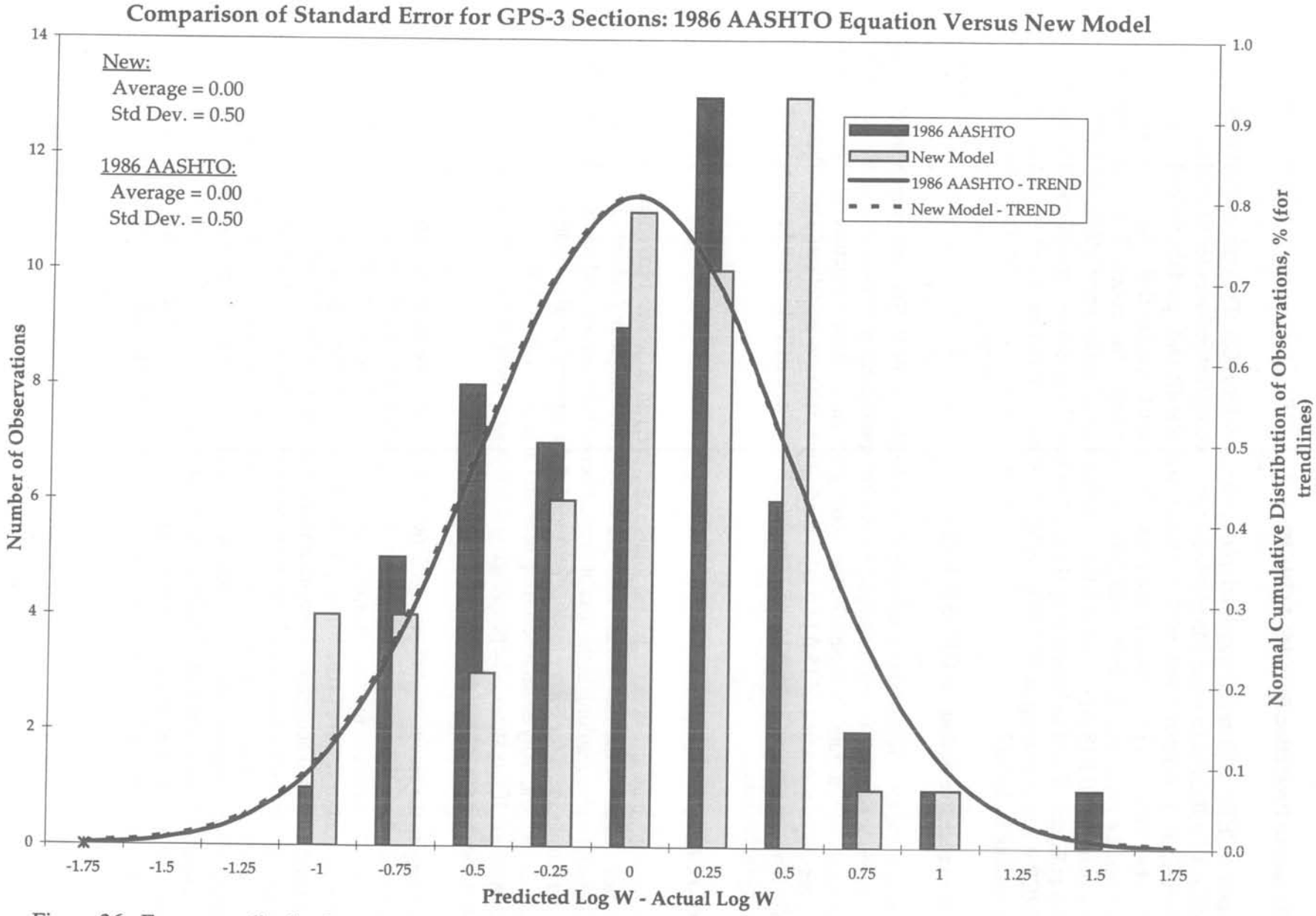

Figure 36. Frequency distribution of prediction error (predicted log W - actual log W) for both original AASHO Road Test model and new NCHRP 1-30 model.

Performance Prediction for GPS-4 (JRCP)

The new NCHRP 1-30 model was developed specifically for JPCP. The only way in which it can be utilized for JRCP is to select a hypothetical joint spacing that provides for an unbiased log W prediction. As illustrated in Figure 37, the model dramatically underpredicts the performance of JRCP when the actual joint spacings are used. This is due to the fact that long joint spacings for JRCP produce unrealistically high curling stresses according to the model. When a hypothetical joint spacing of 30 ft [9 m] is assumed, the model produces unbiased predictions for JRCP as shown in Figure 38 and as indicated by the paired t-test. Thus, the new model could be utilized for JRCP if a joint spacing of 30 ft [9 m] is input. Note that this does not need to be the actual joint spacing in the field.

Performance Prediction for GPS-5 (CRCP)

The new NCHRP 1-30 model was developed specifically for JPCP. The only way in which it can be utilized for CRCP is to select a hypothetical joint spacing that provides for an unbiased log W prediction. As illustrated in Figure 39, the model gives an unbiased prediction for CRCP when a hypothetical joint spacing of 15 ft [4.6 m] is used. Thus, the new model could be utilized for CRCP if a joint spacing of 15 ft [4.6 m] is used. Of course, CRCP does not have any joint spacing in the field.

Corner Stress Evaluation for Undoweled GPS-3 Sections

Slab cracking may also occur near slab joints and corners in undoweled pavements subjected to significant negative thermal and moisture gradients. These negative gradients cause an upward curling of the slab resulting in the loss of support beneath the corners and joints of the slab. The critical tensile stress for corner loading is located at the top surface of the slab, often along the longitudinal joint. Any erosion occurring beneath the joint or corner will cause this stress to increase also. If this stress is large enough and is repeated enough times, corner, diagonal, or even transverse cracks will develop.

According to the recommendations in NCHRP 1-30 for undoweled pavements, a design check is conducted where the maximum top surface stresses were calculated for 76 undoweled GPS-3 sections. The effect of moisture warping was accounted for by an equivalent temperature gradient equal to -1°F/in [-0.02°C/mm], which was added to the negative effective temperature gradient determined according to recommendations given in NCHRP 1-30. The maximum top surface stresses were found to be lower than the maximum bottom midslab stresses (with positive temperature gradient) for all but two sections. It was also observed that very few corner cracks have occurred in any of these 76 sections, which tends to confirm the stress analysis check. However, if erosion occurs in addition to the negative gradients, then the critical stress on the top of the slab will increase and could lead to rapid cracking. Critical conditions where this loading situation is crucial are for thin undoweled jointed plain slabs with stiff bases in hot, dry climates.

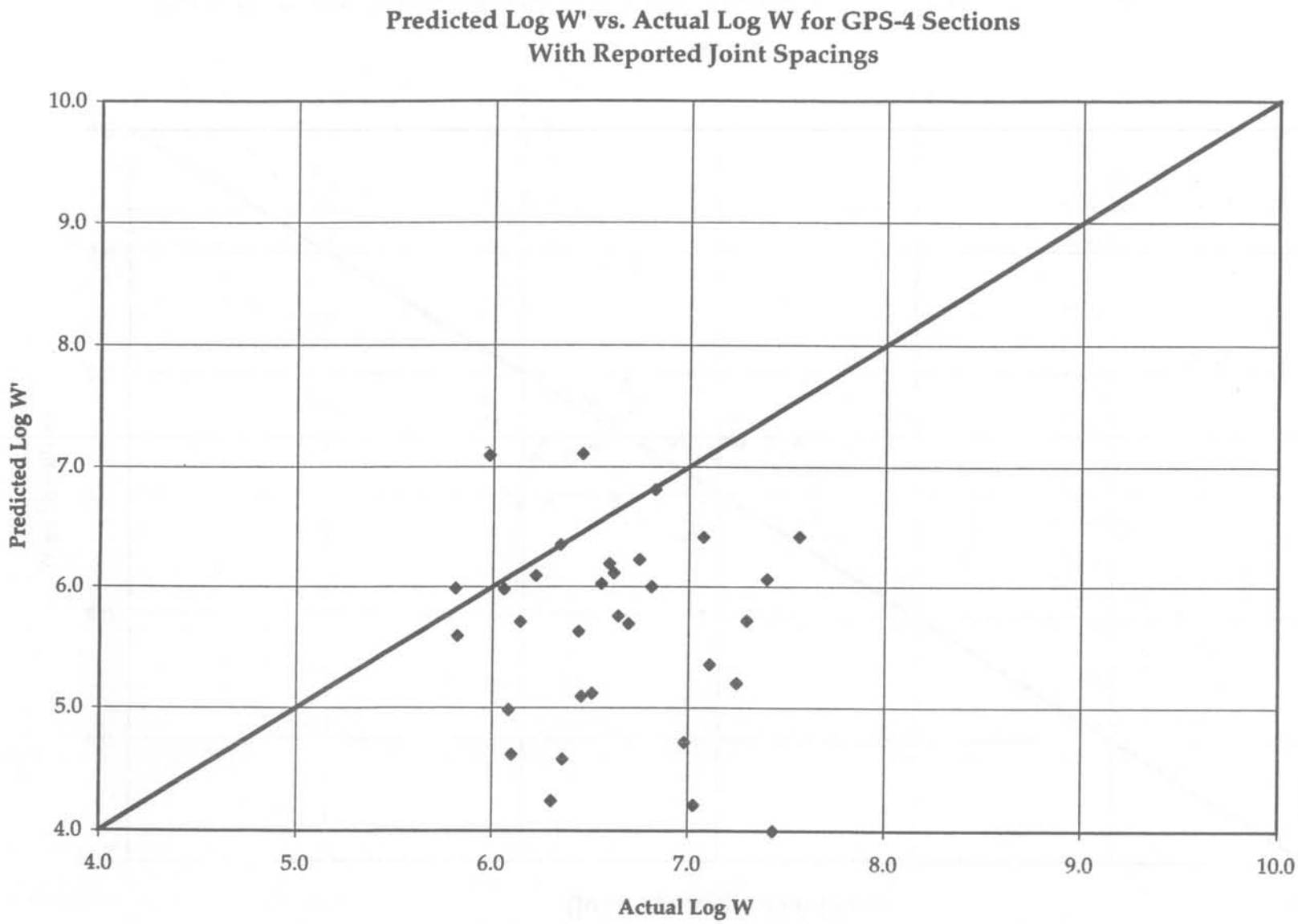

Figure 37. Predicted versus actual log W for GPS-4 using actual joint spacings.

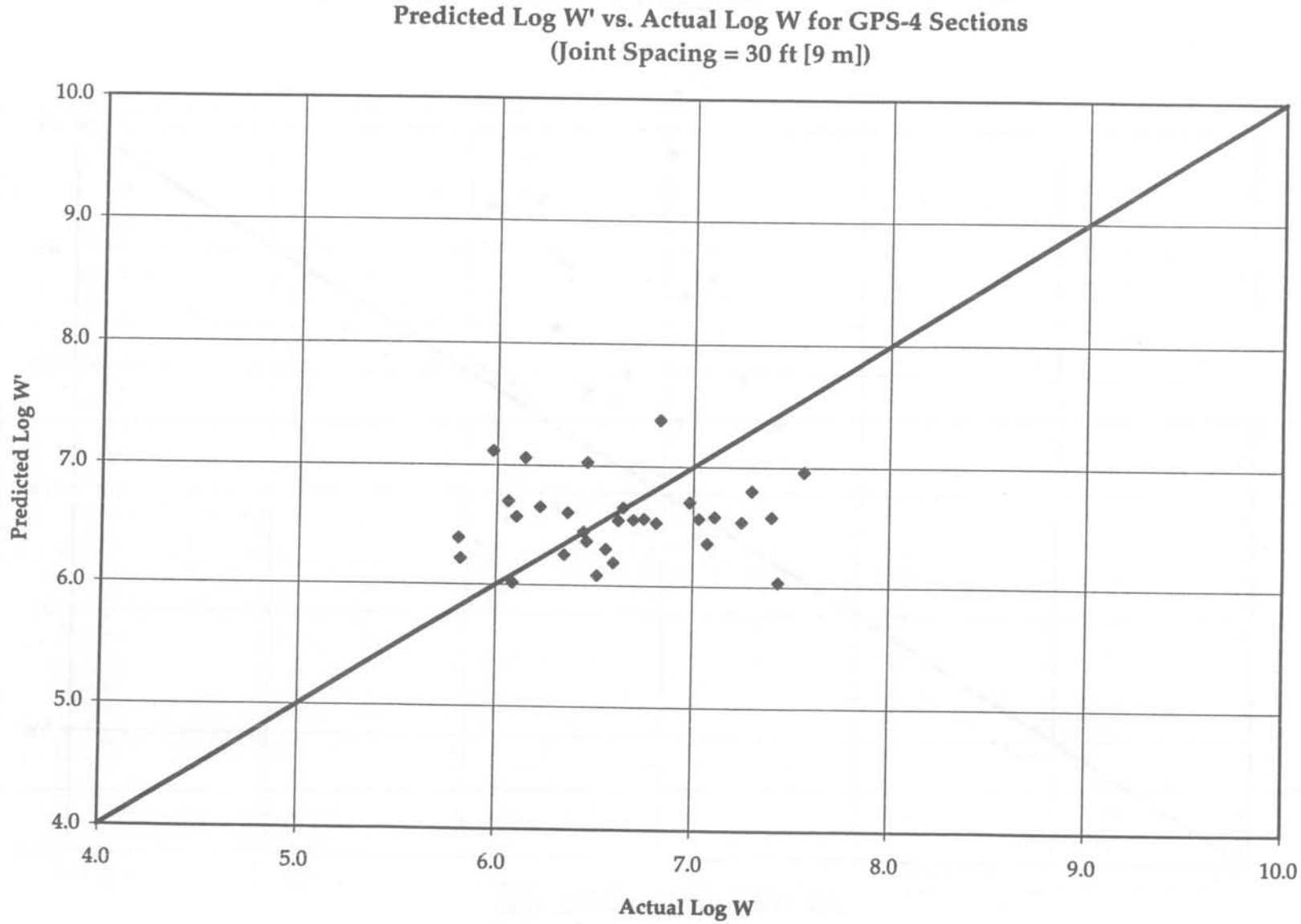

Figure 38. Predicted versus actual log W for GPS-4 using hypothetical 30-ft [9-m] joint spacing.

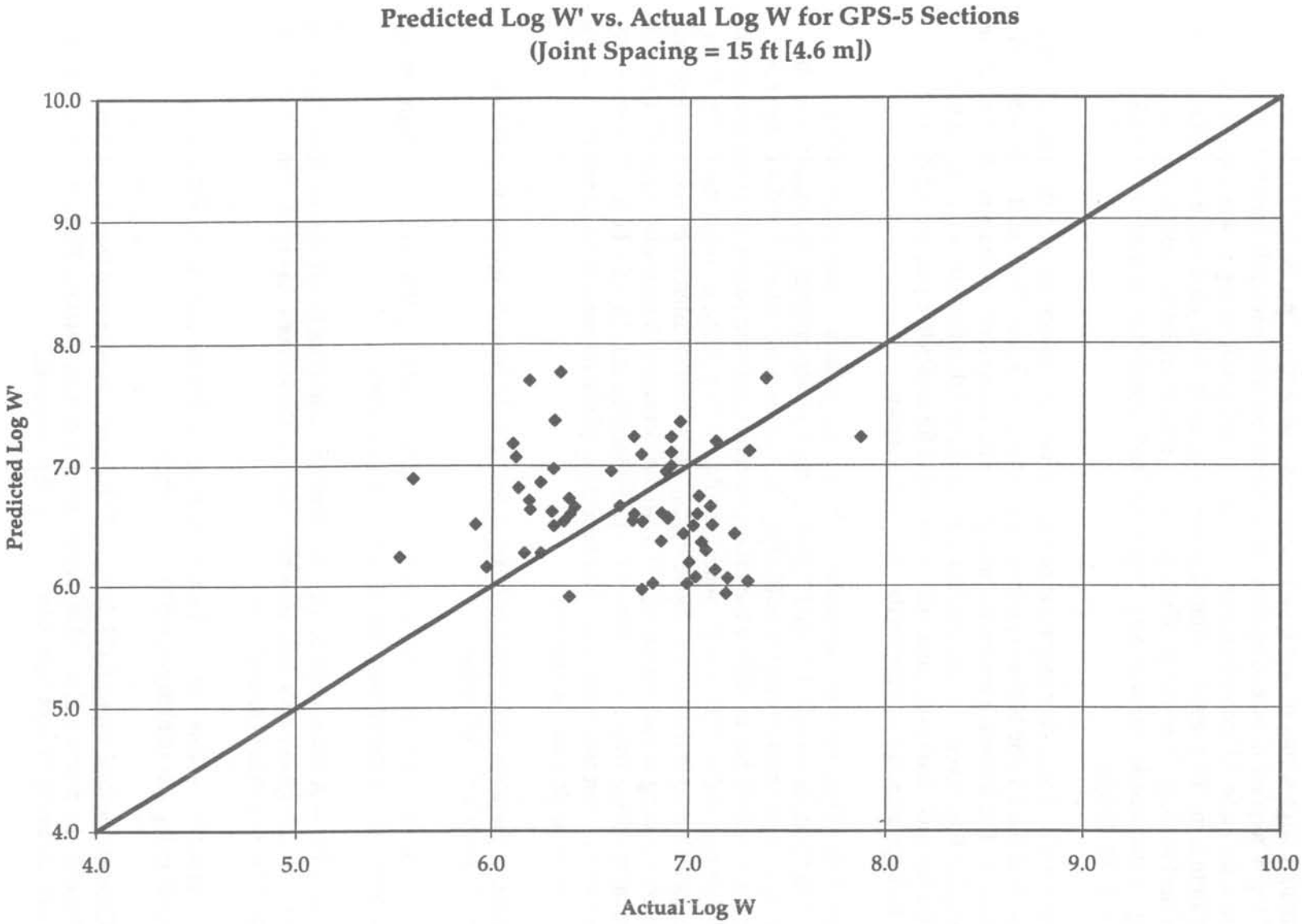

Figure 39. Predicted versus actual log W for GPS-5 using hypothetical 15-ft [4.6-m] joint spacing.

Variability Components of Model Prediction

The seemingly large scatter of data points on the previous plots of "predicted" log W versus "actual" log W requires more explanation. A statistical test was previously used to help determine if the mean difference between actual log W and predicted log W was significantly different from zero. This report section evaluates the magnitude of variation in predicting log W for individual sections. Knowledge of this prediction error is important in pavement design for selecting the standard deviation of performance and traffic prediction as used in the AASHTO Guide reliability design.

There are actually at least four major components of variation associated with the overall scatter of points about the 1:1 line between predicted and actual log W, and these need to be identified and explained. The following represents an approximate analysis of the components of variation. To accomplish this, several estimations had to be made, and thus the results should not be considered as exact. However, these results are useful for illustrative purposes in trying to explain the large amount of scatter on the many plots shown.

(1) Traffic Estimation: Perhaps the easiest component of variation to understand is that associated with the so-called "actual" ESALs, which are accumulated historically from the opening of a pavement section to traffic (V_t). The estimate of "actual" ESALs is dependent on many variables that are difficult to estimate over a multi-year period, including volumes of each axle type and weight over the years, lane distribution of trucks (proportion of trucks in each classification in the outer traffic lane), and directional distribution of trucks (proportion of trucks traveling in each direction). The error associated with estimating "actual" historical cumulative ESALs over many years of the LTPP sections may be quite large. This error may be reduced as increased monitoring data become available for these sections and the historical and monitoring data can be matched.

Components of variation associated with "predicted" ESALs from the prediction model (see Equation 20) include the following:

(2) Errors associated with estimating each design input for each LTPP section (V_i). Some errors associated with selected design inputs include, for example:

Initial P1 — A mean value of 4.25 was used for all sections based on previous information from state highway agencies. However, many of the sections may have been constructed to different levels of smoothness.

Terminal P2 — This value was estimated based on IRI measurements, and a general relationship was used to convert to serviceability.

Concrete flexural strength (28 days) — This value was estimated from a few cores cut from the pavement and tested in indirect tension or compression. Then, the results were back-casted to 28 days from whatever age they were cut.

The k-value of subgrade — This was section mean backcalculated from FWD measurements taken during one season of the year and divided by 2 to estimate the proper static k-value for input.

(3) Random or normal variation between the performance of supposedly identical replicate sections (similar to the variation of strength between two replicate concrete specimens). The causes of this random variation are not usually known (some are known in general and include such items as variation caused by construction processes and materials changes), but can be estimated from replicate section performance data (V_r).

(4) Inability of the model to predict actual pavement performance (serviceability, in this case) due to deficiencies in the model. This is the real model associated error in prediction (V_m). The relatively simple function form of the model does not, of course, represent completely the real pavement behavior under load and climate.

These components of variance can be mathematically expressed as follows (log to base 10):

Prediction Error = Log{Actual ESALs} - Log{Predicted ESALs}

Variance {Prediction Error} = Variance Log{Actual ESALs} +
Variance Log{Predicted ESALs} +
Co-variance {Log(Actual ESALs), Log(Predicted ESALs)}

or: $V_e = V_t + V_p - 2\ r\ Sqrt(V_a)*Sqrt(V_p)$ [24]

where:

V_e = Total variance of prediction (the standard error of the estimate associated with the "actual" log [ESALs] versus "predicted" log [ESALs] as shown in Figure 36 was 0.50 [a standard deviation similar to that recommended in the AASHTO Guide for traffic and performance]; therefore, $V_e = 0.5 * 0.5 = 0.25$).

V_t = Variance of estimating historical ESALs (the error in prediction of traffic used was assumed to be similar to that recommended in the AASHTO Guide, or $V_t = 0.09$).

V_p = Variance of prediction model that includes $V_i + V_r + V_m$.

V_i = Variance caused by estimating model inputs (a variance analysis of the performance model Equation 20, assuming typical variances for each input, gives $V_i = 0.07$).

V_r = Variance due to replication (this variance is from natural variation between replicate sections and was estimated from AASHO Road Test replicate sections to be $V_r = 0.06$).

V_m = Variance due to actual model deficiencies (solved from above equation) = 0.10.

r = Correlation coefficient, 0.25.

The implications of the values of these components of variance can be illustrated as follows. These results are based on observations that the error of predicted log W vs. actual log W shows

an approximately normal distribution (see Figure 36). It is typical for the fatigue life of replicate concrete specimens to be approximately log normally distributed.

Historical ESALs estimate error:
Standard deviation of prediction of historical ESALs = Sqrt(0.09) = 0.30
If the mean ESALs were estimated to be 10 million (using the best estimates of each input), then the 68 percent confidence limits around this value would be approximately
log (10,000,000) ± 0.30 = 7.00 ± 0.30 = 6.70 to 7.30, or 5 to 20 million.

Replication variation only:
Standard deviation of prediction of replication = Sqrt(0.06) = 0.24
If the mean ESALs were estimated to be 10 million (using mean inputs to model), then the 68 percent confidence limits around this value would be approximately
log (10,000,000) ± 0.24 = 7.00 ± 0.24 = 6.76 to 7.24, or 6 to 17 million.

Model error variation only:
Standard deviation of prediction due to model error = Sqrt(0.10) = 0.32
If the mean ESALs were estimated to be 10 million (using best estimates for each input), then the 68 percent confidence limits around this value would be approximately
log(10,000,000) ± 0.32 = 7.00 ± 0.32 = 6.68 to 7.32, or 5 to 21 million.

Thus, the total scatter of data in any of the "actual" versus "predicted" ESAL plots should be considered as consisting of several components of variation, including estimation of the historical ESALs (horizontal axis), estimation of true inputs to the model for each section (vertical axis), random differences in performance between sections due to unknown replication error (vertical axis), and true lack of ability of the model to represent pavement performance (vertical axis). These components of variance can be broken down into percentages of the total variation (V_e) as follows:

Variance Component	**Estimated Variance**	**Percent of Total**
ESAL Estimation, V_t	0.09	28
Input Estimation, V_i	0.07	22
Random Variation, V_r	0.06	19
Model Error, V_m	0.10	31
Total, V_e	0.32	100

As stated in the beginning of this section, the preceding analysis of the components of variation of the performance model is approximate, and the actual values should only be considered as rough estimates. It does point out that, for example, an improvement in estimation of historical ESALs would clearly reduce the scatter on any of the figures, as would an improvement of estimation of inputs. These variations are important because they all need to be considered in determining the overall standard deviation for pavement design reliability using the new model. The model error is the most important component of variation insofar as what needs to be reduced through improved modeling in the future.